DOPPLER FREE ENERGY RELEASE SPECTROSCOPY

by

P. Baltzer, M. Carlsson Göthe, B. Wannberg, and L. Karlsson.

Department of Physics, Uppsala University
Box 530, S-751 21 Uppsala
SWEDEN

UUIP-1231 Oct 1990

Abstract

A new method for measurement of kinetic energy release in the dissociation of doubly ionized free molecules is presented. The two fragments are detected in coincidence, and the thermal motion of the dissociating molecule is corrected for in real time by accurate measurement of the time difference between the fragments within the coincidence window. The low overall detection probability often encountered in coincidence experiments is avoided by taking advantage of the strongly peaked angular distribution from the two particle decay. Preliminary measurements on the doubly charged ions of O_2 and HD are presented. The experiments reported here constitute a feasibility study, and methods to enhance the information rate are discussed.

INTRODUCTION.

As a complement to UV photoelectron and Auger electron spectroscopies, we use a polarity-reverted electrostatic electron spectrometer to study the ion kinetic energy release spectra from some simple molecules. Studies have been performed on HCl/HBr [2], HI [3] and O_2 [4]. These investigations have resulted in an increased knowledge in molecular dynamics, *e.g.* for doubly ionized states.

UV photoelectron spectra and in certain cases Auger electron spectra routinely give a resolution sufficient to resolve vibrational progressions. The resolution is typically 10-50 meV. This level of resolution is not found in the ion spectra. The resolution in these spectra is limited by the thermal motion of the dissociating molecule, which has a very large influence on the kinetic energy of a fragment ion. This process is generally referred to as Doppler broadening in analogy with the optical case.The Doppler broadening is in the range of $\approx$0.1–1eV whereas the electrostatic spectrometer itself is capable of a resolution below 10 meV. In fact, the lower resolution limit at 0.1 eV was previously reached only in the extreme case of the HI molecule where one vibrational progression was resolved. The rich structure observed even at this limited resolution clearly motivates further efforts to improve the resolution.

In this paper we describe a new coincidence experiment , which can be applied to the case of a doubly ionized molecule, dissociating into two charged fragments. In this experiment the center of mass movement of the dissociating molecule is corrected for in real time. The compensation should theoretically permit a resolution in ion fragment spectra of the same order of magnitude as in UV photoelectron spectra.

A feasibility study was performed using an electrostatic photoelectron spectrometer described elsewhere [1]. This instrument was augmented with a drift tube of 100 mm length with a channeltron detector in the direction opposite to the electrostatic analyser. The setup is schematically outlined in Fig. 1. Furthermore, a new experiment control and acquisition system has been developed complementing the old data acquisition system previously reported. The detector in the electrostatic instrument was reconstructed to allow time resolved electronic readout, while the former phosphorescent screen is retained since this screen is an invaluable tool for checking that the spectrometer operates properly by inspection of the actual lineshape. The time resolved readout was,however, limited to only one energy channel at a time, with severe limitations in countrate as a consequense. The acquisition of a spectrum took several days to get sufficient statistics. The technique would work as well with a multichannel detector, provided time resolved readout is available. We discuss below the possibilities to enhance the sensitivity with some orders of magnitude.

THEORY

The energy resolution in ion fragment spectroscopy is normally limited by the Doppler broadening caused by the thermal motion of the initial molecules. For a molecule dissociating into two fragments of masses m_A and m_B with a total energy release E_F at a temperature T, the FWHM of the Doppler profile in either fragment is given by

$$\frac{4}{m_A+m_B}\sqrt{ln\,2\,m_A\,m_B\,E_F\,kT}$$

The worst case occurs when $m_A=m_B$, where the broadening at $E_F=10$ eV becomes 0.86 eV at room temperature. When $m_B<<m_A$, the broadening for fragment B becomes approximatively

$$4\sqrt{ln\,2\,\frac{m_B}{m_A}\,E_F\,kT}$$

The Doppler broadening can be reduced by lowering of the temperature of the sample, as can be achieved using a supersonic molecular beam perpendicular to the direction of observation. Since the broadening varies as the square root of the temperature, an efficient improvement of the resolution requires very low temperatures, which in practice involves large expansion ratios in the beam, i.e. very large gas fluxes with the corresponding requirements of pumping.

In order to determine the actual energy released in the dissociation, independent of the thermal energy, the kinetic energies of both fragments have to be measured. Using this information, it is possible to deduce both the fragmentation energy and the thermal energy. This requires a coincidence arrangement, where for intensity reasons at least one of the channels has to be able to detect a particle and measure its energy whenever this is within a certain energy range. It should be noted, that only dissociations leading to two charged fragments will be observed in such measurements. Thus, one could in principle use two particle spectrometers of a dispersive type (e.g. hemispherical sector) where at least one has a multichannel detector. Two time-of-flight spectrometers in coincidence could also be used. If the excitation is pulsed, the measurement of the energies in the two channels is then straight-forward. In this paper, we describe in some detail how the correction for the initial thermal velocity can be achieved with continuous excitation. The crucial points are the choice of the coincidence criterium, the accurate timing of events fulfilling this criterium, and the real-time energy correction algorithm.

In the present set-up, one of the channels (B) is an electrostatic hemispherical spectrometer, which has been modified for use as an ion spectrometer [1]. The other channel (A) is a simple time-of-flight tube equipped with a channeltron detector, mounted at 180° from the entrance direction to the spectrometer. To provide accurate timing, the detector in the hemispherical analyser has been modified as described below.

The ions detected in channel B have a well-defined energy E_B and a corresponding initial velocity w_B (cf. Fig. 2 for notations), and hence their transfer time through the lens and the analyser can be calculated with high accuracy, using the known variation of their kinetic energy throughout the system. This provides a time base for the time-of-flight channel. If an ion has been detected in that channel within a certain time interval, to be discussed below, its velocity w_A can be calculated. The fragment velocities in the center-of -mass system, v_A and v_B and the thermal velocity component v_T along the direction into channel B and hence the released energy can then be calculated using the relations

$$w_A = v_A - v_T$$
$$w_B = v_B + v_T$$

and from conservation of momentum

$$v_B = \frac{m_A\, v_A}{m_B}$$

Thus,

$$v_A = \frac{(w_A + w_B)}{\left(1 + \frac{m_A}{m_B}\right)}$$

The real time correction of the fragment energies, although based on this equation, proceeds in a slightly different way in order to provide a rapid algorithm. The directly measured quantity is the time difference t_{DIFF} between two coincident fragments. This time difference is measured as a number of discrete steps with a well-defined length (200 ns). The time difference corresponding to the dissociation of a molecule without thermal motion is calculated just once for each setting of the electrostatic spectrometer, and so is the energy correction corresponding to one time step deviation between the actual time difference and this reference time difference. For the small time deviations of interest here, the energy correction is to sufficiently good accuracy a linear function of the time deviation. The energy correction for each event, obtained as the product of the energy correction per time step and the number of time steps, is applied to the measured fragment energy before the event is added to its proper energy channel in the spectrum.

The size of the coincidence window can be chosen to optimize the ratio between real and random coincidences. Obviously, most real coincidences will occur with deviations from the reference time difference corresponding to initial velocities within $\approx \pm v_T$, where

$$(m_A + m_B)\frac{v_T^2}{2} = kT$$

and the coincidence window should be of the order of magnitude of this deviation. Using a smaller window a large proportion of real coincidences will be discarded, while a too large window increases the probability of spurious coincidences.

So far, only the initial velocity component along the direction of observation has been discussed. The perpendicular component has to be considered from two points of view. One effect is that the fragments are not emitted in opposite directions in the laboratory system. In the present set-up, the acceptance solid angle of the B channel (the hemispherical analyser) is very small compared to that of the A channel. If one fragment is observed in channel B, the other fragment is distributed around the opposite direction within a lobe with an angular FWHM given approximatively by

$$\theta = 2\ tan^{-1}\left\{\left(1+\frac{m_B}{m_A}\right)\frac{1}{\sqrt{\frac{m_A}{m_B}\frac{E_F}{kT\ ln\ 2}-1}}\right\}$$

In the homonuclear case this gives

$$\theta = 2\ tan^{-1}\frac{2}{\sqrt{\frac{E_F}{kT\ ln\ 2}-1}}$$

while in the other extreme case, when $m_B/m_A < kTln2/E_F$ the A fragment may have any direction. For homonuclear molecules, this solid angle is not very much larger than the acceptance of the A channel, so in this case the coincidence losses are small.

The energy associated with the perpendicular velocity component is not measured, and thus gives a contribution to the energy resolution. An analysis of this effect shows that it is largest in the homonuclear case, and if the A channel were to accept the full angular lobe from the dissociation, the line broadening from this source is of the order kT/2. Compared to the energy resolution of the hemispherical analyser and other contributions to the line width this can normally be neglected as kT at room temperature is 25 meV.

Besides the energy resolution of the hemispherical analyser, there are a number of other contributions to the line width. The most important of these are:

- The finite time resolution.
- Differences in flight times for particles with different trajectories in either channel.
- The uncertainty in start position due to a finite size of the excitation region.

The energy difference corresponding to the clock period t_c is given by

$$\frac{\Delta E_F}{E_F} = \frac{2\sqrt{2}}{L}\frac{m_B^2}{(m_A+m_B)^2}\sqrt{\frac{m_A\ m_B\ E_F}{m_A+m_B}}\ t_c$$

With an acceptance semiangle θ of the time-of-flight tube, the relative difference in length between the central and peripheral trajectories is $\theta^2/2$, leading to a relative error in the total release energy of approximately

$$\frac{\Delta E_F}{E_F} = \frac{\theta^2}{2}\frac{m_B}{m_A}$$

The length z of the excitation volume is less than 0.5 mm, while the time-of-flight tube is L=100 mm long. The relative error in energy from this source is given by

$$\frac{\Delta E_F}{E_F} = 2\left(\frac{Z}{L}\right)\left(\frac{m_B}{m_A}\right)$$

where the factor 2 comes from the addition of the errors for the two fragments.

EXPERIMENTAL DETAILS.

Recent reconstruction.

To make the new ion coincidence experiment possible the spectrometer has been reconstructed. This consisted mainly of the new time-of-flight tube, new detection equipment for the two flight channels, and a new data acquisition system. Some minor problems discovered in the old design have also been addressed.

The detector.

The electron spectrometer used is equipped with a multichannel detector composed of two MCP plates in Chevron arrangement and a P20 phosphor screen, which in turn is viewed by a CCD TV-camera. Due to the serial signal transmission from a CCD, it can not be used for fast time-resolved experiments like the present. To enable direct electronic readout of one energy channel, a 0.1 mm copper wire was inserted between the MCP and the screen. This wire was then connected to a potential slightly above the undisturbed potential value at the appropriate distance from the MCP. This resulted in a minimum of geometric image distortion near the wire, but permitted absorption of the full charge emitted from the MCP in a 0.1 mm strip below the wire. A mesh in front of the MCP package enables the application of a variable acceleration voltage to the front of the first MCP without distorting the field at the end of the analyzer. An accelerating voltage of about 1 kV was found appropriate for this purpose. Test runs with UV-excited electron spectra showed a resolution of about 40 meV at an analyzer pass energy of 50 eV and 0.2 mm entrance slit width.

A note on the wire material choice should be passed. It was found, that the native oxide layer present on metals such as tungsten and nickel withstood a potential above 1 kV, leading to a gradual charging in a matter of minutes leading to progressively weaker signals and changes in the shadow image seen on the screen. On the other hand, copper wires showed no such effects even when used directly from the roll without any cleaning except alcohol rinsing.

Figure 3 shows a schematic drawing of the detector unit. The numbers in the following description refer to the component numbering in figure 3.

The detector unit is housed in a stainless steel container (1) with a silver-epoxy glued high transmission gold mesh (2). The mesh is spray-coated with a colloidal graphite suspension in isopropanol. The various detector parts are stacked in the container in the following order: First MCP (3), second MCP (4), single channel wire (5), and phosphor screen (6), washer (7) and a lid (8). The assembly is compressed by three screws (9). The electrical connection to the MCPs, the wire, and the phosphor screen is obtained by stainless steel washers (10,11,12,13) isolated by ceramic rings (14). The connection washers are isolated from the surrounding container by a Teflon layer (15). The detector voltages are supplied to the washers via male pin connectors (16) soldered directly to the washers. The detector unit is mounted to the spectrometer by two screws (17).

The sample gas cell.

The new gas cell was designed with an additional stage of differential pumping to further reduce the analyzer pressure, since the collision cross sections for ions are an order of magnitude higher than for electrons of the same kinetic energies. The gas cell is mounted at 90° angle to the lens.

The gas cell consists of an outer cell, electrically connected to the first lens element, and an electrically isolated inner cell. The two cells define the first differential pumping stage. A adjustable voltage may be applied between the inner and outer cell to retard or accelerate the particles. Both cells are cylindrical, each having two opposite slits of 1 x 6 mm in a plane perpendicular to the axis. The inner cell has an inner radius of 8 mm and the spacing between the cells is 2 mm.

The reason to shift the gas cell potential with respect to ground was primarily to suppress the very high ion current coming from molecules that just have lost one electron without dissociating and thus still travel at the thermal velocity. This is a much more probable process than the dissociation in two charged fragments and will saturate the detection system if not suppressed. However, as discussed below, it was found to be more advantageous to perform this suppression after the time of flight tube.

The differential pumping of the gas cell now gives the possibility to run at a gas cell pressure of 20mTorr with an analyzer pressure of $<10^{-5}$ torr.

The excitation is made with a continuous 300 eV electron gun with a beam diameter in the sample gas cell of <0.5 mm.

The Time-of-Flight tube.

The time of flight tube simply consists of a 100 mm long graphite coated aluminum tube, with an entrance slit of 2x10 mm and a 30 mm diameter exit aperture which is covered by a mesh. In order to collect the ions into the 5 mm diameter entrance of the channeltron, a focusing electrode, also close to ground potential, is placed between this mesh and the channeltron. This focussing electrode has the shape of a cup which is closed by a mesh less than 1 mm from the mesh on the time of flight tube. Figure 4 shows these details. The tube is clamped to a standard CF flange by a ring allowing sidewise adjustment. The tube is separately pumped by a turbo pump.

The channeltron is connected with the output at ground potential and with the input at approximately -3 kV, giving high efficiency counting of positive ions. The ions are accelerated within a short distance after the second mesh to a sufficiently high velocity that differences in flight times from different positions on the 30 mm opening can be neglected.

When running the experiment we found that the time-of-flight channel was almost saturated even at moderate pressures and electron gun intensities. To reduce the number of low energy ions, we first tried to retard the low energy ions between the inner and outer gas cells as mentioned above. This did not eliminate all low energy ions, however, since some of these were generated outside the gas cell. The change in velocity shortly after the exit from the gas cell also introduced another parameter in the calculation of flight times. To solve these problems, we instead have chosen to carry out the retardation between the two abovementioned meshes. The distance between the meshes is below 1 mm, so the influence on the time of flight can be ignored. The voltage between them may be varied from 0 to+12 V. The voltage in practice is set to about approximately 1 V below the lowest ion energy of interest in order to eliminate as much uninteresting ions as possible.

THE EXPERIMENT CONTROL AND DATA ACQUISITION SYSTEM.

General outline.

The measurement is performed by analyzing the information from the two channels; the electrostatic spectrometer channel (B), and the time-of-flight tube (A) channel. Two modes of operation are used. In one mode, the electrostatic spectrometer voltages are set up to accept a certain fixed kinetic energy and the corresponding time difference spectrum is acquired. In the second mode, which is the normal operation mode, the electrostatic spectrometer is slowly swept over the energy range of interest. For each energy step the time differences are used in conjunction with the spectrometer voltage information to calculate the correct energy position for each event. An energy spectrum is built from the subsequent addition of these events over any desired time.

The coincidence measurement instrumentation consists of three stages. First, the signals from the MCP wire detector and the CEM are amplified in two pre-amplifiers. Second, the pulses from the pre-amplifiers are fed to the coincidence analyzer.Third, those events that are accepted as true coincidences are transferred to a Macintosh Plus computer running the coincidence control program. The Macintosh hosted program converts the time difference information, with knowledge of the current electrostatic spectrometer voltages, to a fragment energy value, adds the event energy to its appropriate energy channel and presents the collected spectrum on the Macintosh screen.

In the sections below the various parts and algorithms of the instrumentation are presented.

The pre-amplifiers.

Both preamplifiers are low-cost charge sensitive amplifiers with a delay-line differentiator circuit producing 130 ns square pulses with low pileup problems. The input is fully protected against HV flashover in the detector. The output feeds a terminated coaxial cable with CMOS-compatible signal leves.
The complete circuit diagram of the pre-amplifiers is presented in Figure 5.

The coincidence analyzer card.

The coincidence analyzer is implemented as two separate cards; the time base card, and the microprocessor coincidence analyzer card.

The first card, in the data flow direction, is used to generate a time mark of a detected event. The time base is created by a quartz controlled 14-bit counter running at 5 MHz. The counter was implemented using four 74ALS163 synchronous 4-bit counters. A pulse from either pre-amplifier transfers the current counter value to a 512 word FIFO buffer (two IDT7201). The counter output and the FIFO register write cycle is controlled by a JK flip-flop synchronizer. Apart from detected ions, each counter zero wrap-around is transferred. This is referred to as a heart-beat and is used to overcome the wrap-around ambiguity. The time between heart-beats is 3.28 ms. Bits 14 and 15 are used to label the event as "A" or "B". The label is used by the coincidence analyzer algorithm. Events occuring at a heart-beat are discarded to simplify the search routine. Table 1 below shows this labeling.

The coincidence analyzer algorithm runs on a microprocessor card manufactured by GammaData Mätteknik AB. The card is equipped with a NEC70208, a 8086 compatible microcontroller with on-chip timers and parallell- and serial ports. Furthermore, the card features; 32 kByte ROM, 32 kByte RAM, a 16 bit parallel port and a serial port. The output from the FIFO buffer is connected to the parallell port. The FIFO buffer write control and parallel buffer handshake is controlled by JK flip-flops. A hardware, 'not empty', signal from the buffer automatically start the transfer sequence. The input - and output logic of the FIFO registers are fully parallel.

The algorithm of the coincidence analyzer is quite simple. It is controlled by two parameters, DIFF and DELTA, calculated by and transferred from the coincidence control program at the beginning of each energy step. DIFF represents the algebraiclly smallest accepted value for the time difference, t_A-t_B, between channel A and B. DELTA extends the coincidence window in the positive direction. Figure 6 exemplifies the algorithm and the DIFF and DELTA parameters. Looking at the figure, one sees that four events have been registered since the last heart-beat, the B events 9130, 8995 and1138, and the current A event at 9500. The DIFF parameter has in this case been set to 500 and the DELTA parameter (always positive) to 10 extending the window to 509. One sees that only the second B event at 8995 falls within this window. The A event at 9500 and the B event at 8995 are thus considered a coincidence pair, the time difference TIME_DIFF is calculated to be 505 and is immediately transferred over the serial link to the coincidence control program in the Macintosh. It should be remarked that the time order between coincident events in this example is not the one encountered for homonuclear molecules. In that case, the transfer time in the B channel is always longer than in the A channel, making the appropriate value of DIFF negative.

The implementation of the algorithm involves the handling of two cyclic tables containing event time markers for each channel. A new event starts the scanning in the opposite table to search for a coincidence inside the specified time difference window. Heartbeats are entered as zeroes into both tables. A scan is stopped when the second heartbeat event is found in the table. The algorithm is written in assembly code and accepts an event frequency of about 10^3 events/s before saturating. Note that due to the FIFO register, saturation occurs only when the average time between the events is smaller than the time required for the search algorithm. If the saturation rate is exceeded, a LED connected to the FULL flag of the FIFO is lit, and a reset has to be performed.

The coincidence analyzer card is fully controlled from the coincidence control program. It communicates over a 19200 Baud serial link. This imposes no limitation as the typical data rate in the experiment is 0.1 to 1 coincidence per second. The command set includes sending parameters, starting and stopping the data acquisition, and a reset command. The reset command performs a hardware reset on both the digital- and microprocessor cards. The complete circuit diagrams of the time base card is presented in Figure 7. Table 2 summarizes the coincidence analyzer card command set.

The coincidence control and data acquisition program.

One of the basic design ideas for the coincidence control and data acquisition system was to reuse as much of the normal instrumentation as possible. It was decided to run the coincidence control program in a separate Macintosh computer collecting information both from the coincidence analyzer and the IBM compatible computer used for spectrometer control . The coincidence controller is a slave unit to the spectrometer controller, and the spectrometer control program transfers the necessary data to the co-

incidence controller. When running, the IBM spectrometer controller collects an ordinary non-corrected spectrum through the TV-camera simultaneously with the coincidence spectrum.

Figure 8 shows a schematic drawing of the ion coincidence spectrometer system with its two experiment control computers. The coincidence controller is connected, via the printer port, to the GPIB bus using a GPIB-422 CT Serial GPIB Controler by National Instruments. A driver program, written in IBCL (Instrument Bus Control Language), makes the unit a transparent GPIB-Serial converter. The coincidence controller is also connected, via the modem port, to the coincidence analyzer cards.

The coincidence control and data acquisition program has three tasks. First, to collect, analyze, and store the coincidence data sent by the coincidence analyzer card. Second, to monitor the current spectrometer voltages and running status. Third, to offer a user interface including presentation of the collected data, and the status of the experiment.

One of the major problems in implementing a single-computer data acquisition program is to allow instant response to all events, created by both the instrumentation and the user. This problem is accentuated in this experiment where calculations have to be performed on each accepted coincidence.

The coincidence control program was written in THINK's Lightspeed Pascal 2.0. The user interface was prototyped using the automatic code generator Prototyper™ by SmethersBarnes and follows the guidelines for Macintosh programs. The program is implemented using the basic program structure used for event driven systems, such as the Macintosh. It consist of a main event and update loop. The Macintosh OS handles all event queuing and the low level IO services. No interrupt service is required by the program. Events are handled in sequence by separate handlers. Figure 9 gives a brief view of the software components, or units, integrated in the program.

The program may operate in three major modes; a fixed data acquisition test mode, a swept data acquisition mode, and a 'old spectrum' display mode.

The spectrum display mode is used for preliminary analysis of the spectral results. All spectra are stored in the CRUNCH format used at the laboratory [5].

The fixed data acquisition mode is intended as an optimization mode. The voltages of the electrostatic analyzer are held constant to accept a certain kinetic energy, and a comparatively large coincidence window is specified, centered at the time difference corresponding to the dissociation of a molecule at rest. The intensity distribution in the coincidence spectrum is then given by the product of the Doppler profile and the dissociation energy spectrum in the vicinity of the chosen energy. The calculation of the time difference between the two channels contains some empirical parameters, intended to correct for inaccuracies in the determination of flight distances and potential distributions, and one purpose of this operation mode is to enable optimisation of these parameters to give the best energy resolution. The control program in this case displays

a spectrum of intensity versus flight time. The parameters to the coincidence analyzer card may be entered in a window. A screen capture of the program running a fixed experiment is shown in Figure 10. Figure 11 shows a typical time difference spectrum of HD. In this case, the fragmentation spectrum does not contain any sharp structures, so only the Doppler profiles appear in the resulting spectrum. The difference in Doppler broadening between the two isotopes is clearly seen. Note that the time difference scale is numbered in counter ticks (1tick = 200ns).

The swept data acquisition mode is the principal mode for data acquisition. This mode performs a complete swept run over a specified energy region. The control is given to the spectrometer control computer and the run parameters are specified using normal procedures. The coincidence control program is given a run command placing the program in an attention state.

A set of GPIB commands has been defined for the communication between the spectrometer and the coincidence controller. The command set includes start and termination of an experiment, a region, and a sweep, transfer of the run parameters, voltage settings, and a step command. Two software components, `GPIB_Handler` and `SpectrometerStateHandler`, have been designed for GPIB command buffering and parsing. Furthermore, the `SpectrometerStateHandler` keeps the state and alarms the `TOF_SerialHandler` when the state changes. This results in the initiation of actions such as changing the parameters used in calculations, transferring and saving of the recorded spectrum, or the termination of an experiment.

For each coincidence registration a calculation has to be performed to correct for its particular Doppler shift. The equations used include the flight distances of the two channels, the atomic weight and charge of the fragments. These parameters may be set using dialog boxes in the program. Figure 12 shows two screen snapshots of these dialog boxes.

During each energy step of the electrostatic spectrometer scan, a temporary spectrum of intensity versus time differences is accumulated. After a finished step, this temporary spectrum is converted to an energy spectrum. It is then added to the final spectrum with an offset for the center channel calculated from the present value of the acceleration voltage in the electrostatic spectrometer. The energies corresponding to other channels are calculated using the energy difference per time step as described above. This conversion and transfer are executed during the period when the voltages in the electrostatic analyzer are changed.

Simulation.

A set of simulations has been performed to check the numerical model used. These simulations were developed using Microsoft Excel for the Macintosh.

The expected time difference and Doppler broadening is calculated for a given dissociation energy. The probable dissociation energies are extracted from known potential curves of the sample under investigation. The calculated numbers are used when assigning the parameters in the fix trimming mode, *cf* Figure 10. When running the experiment a peak is expected to appear near the calculated values.

RESULTS.

The new method was used with the H_2, D_2, HD, CO, O_2 and N_2 diatomic molecules as target gas. The results reported here are only intended to demonstrate the technique. Due to uncertainties in the calibration parameters, the energy scales might be in error with up to 1 eV.

All gases except HD were obtained commercially as high purity laboratory samples. The deuterium was enriched to 99% D_2. The HD, however, had to be prepared in the laboratory using a reaction between lithium hydride and heavy water. When LiH is dissolved in D_2O, the negative hydride ion is immediately reacting with the D_2O, forming gaseous HD and a dissolved OD ion. The process was carried out by addition of liquid D_2O to outgassed LiH residing in an evacuated glass flask, connected to a reservoir by a tube containing phosphorous oxide as a desiccant.

The H_2, D_2 and HD molecules.

The hydrogen molecules were run to check that the anticipated flight time through the electrostatic lens and analyzer were correctly calculated, as these entities are used in the data processing for each coincidence. Due to the extreme simplicity of the doubly ionized hydrogen molecule, two free nuclei where the internuclear distance probability distribution is determined by the well known ground state wavefunction in the neutral molecule, the fragment energy distribution is calculable to a high degree of precision. The result is a gaussianlike distribution with its maximum point at 18.8 eV total energy [6]. The half-intensity points are located at 15.6 eV and 22.8 eV. The D_2 molecule is expected to give a somewhat narrower energy distribution due to the smaller vibrational level spacing which in turn results in a narrower Franck-Condon region.

In the case of HD, the two fragments share the total energy in inverse proportion to their masses, permitting tests on a known structureless distribution to be made at two different kinetic energies. Together with the homonuclear species, this gives four points of calibration for the correction algorithm.

In a numerical simulation using the actual correction equations, the flight time differences and Doppler widths, given in Table 3, were obtained. This table also contains experimental results for comparison.

It should be noted, that the fragment in the analyzer travels most of its path at a constant kinetic energy (50 eV) and that the part of the entrance lens where the kinetic energy is still low has approximately the same length as the time of flight tube, so the time differences for homonuclear molecules are considerably smaller than the total flight time. The minus sign means, that the fragment in the time of flight tube was the first one to arrive. These spectra are shown in Figure 11 and 13.

The O_2 molecule.

Previous investigations and calculations, e.g. [4], have studied the dissociation, via Coulomb explosion, of the doubly ionized oxygen molecule. It was found that the doubly ionized states were created both by direct two-electron emission and by Auger processes. The former process is the dominating one. Six structures were observed in the ion kinetic energy spectrum, *cf* Figure 14. These structures were assigned using CASSCF/MRCCI calculations of the potential curves for the doubly ionized states.

Table 4 summarizes the energies and the assignments of the lines in the coincidence ion spectrum shown in Figure 15. Comparisons are made to the structures reported in ref. [4].

Dissociation processes resulting from singly ionized molecules are suppressed in the coincidence experiment. The dominating structures (1 and 2) in the non-coincidence spectrum, shown in figure 14, are only seen as the small structures (1, 2 and 3) in the coincidence spectrum, shown in figure 15. These processes were assigned as dissociations of singly ionized molecules. Structures corresponding to these dissociations are present at a low intensity in the coincidence spectrum due to the dependence of the number of random coincidences on the total intensity in the B channel. .

CONCLUSIONS AND FUTURE DEVELOPMENT.

The results presented above show that the method is feasible and will make the structure in the kinetic energy spectra accessible for investigation at a new level of resolution. For example, in the O_2 spectrum a narrow feature exists at a fragment energy of 5.4 eV, where the Doppler width at 300 K is 0.9 eV. This feature has a width in fig 15 of 0.25 eV, corresponding to the Doppler broadening at a sample temperature of less than 25 K assuming a negligible width of the structure itself. Since the experiment at its present stage of development suffers from inconveniently low countrate and too many parameters to adjust, a different apparatus is being planned. This will combine multichannel detection in both channels with a symmetric geometry leading to a significant reduction in neccesary variables. The idea is to use a fast pulsed electron gun for the excitation and do the energy analysis in two collinear time of flight tubes. Before the

present study, it was anticipated that the time-dependent plasma potential in the gas cell during the electron pulse would be the resolution-limiting factor in that case. This was based on the experience from high-resolution Auger spectroscopy.According to experience won in this experiment, this factor should not impair the resolution at total true coincidence countrates two orders of magnitude above the present limit, which is due to random coincidence problems.

ACKNOWLEDEGMENT

The support and help from Karl-Göran Görsten at GammaData Mätteknik AB is greatly appreciated.

REFERENCES.

[1] P. Baltzer, B. Wannberg and M. Carlsson-Göthe,
Revi. of Sci. Instr. in print 1990.

[2] P. Baltzer, B. Wannberg, S. Svensson and L. Karlsson.
Uppsala University Institute of Physics Report, UUIP-1190, 1988.

[3] P. Baltzer, L. Karlsson, S. Svensson and B. Wannberg.
Uppsala University Institute of Physics Report, UUIP-1209, 1989.

[4] M. Larsson, P. Baltzer, S. Svensson, B. Wannberg, N. Mårtensson, A. Naves de Brito, N. Correia, M. Keane, M. Carlsson-Göthe and L. Karlsson. J. Phys. B. 23 (1990) 1175-1195.

[5] R.P. Vasques, J.D.Klein, J.J. Barton and F.J. Grunthaner,
J. Electron Spectrosc Rel. Phen., 23 (1981) 63.

[6] K. E. McCulloh and H. M. Rosenstock. J. Chem. Phys 48 (1968) 2084.

TABLES

Table 1. *The event coding from the time base card.*

Bit 0-13 Counter value	**Bit 14** Channel A event	**Bit 15** Channel B event	**Event description**
0	0	0	A heart-beat event. The counter value is ≡ 0.
Any value	1	0	An event in the B, spectrometer, channel.
Any value	0	1	An event in the A, time-of-flight, channel.
Any value	1	1	An event in A and B channel simultaneously.

Table 2. *The command set for the Coincidence analyzer.*

Command name	**Binary code**	**Command description**
ENQ	05 HEX	Inquire the state. Returns ACK.
ACK	06 HEX	Acknowledged. Used as a command response.
NAK	07 HEX	Not Acknowledged. Used as a command response.
STX	02 HEX	Start data acquisition. Returns ACK.
ETX	03 HEX	Stop data acquisition. Returns ACK.
CAN	18 HEX	Cancel and reset both cards.
T	54 HEX T ASCII	Transfer the DIFF parameter. Returns ACK. Sequence: T{DIFF}{CR}
D	44 HEX D ASCII	Transfer the DELTA parameter. Returns ACK. Sequence: D{DELTA}{CR}

Table 3. *The calculated and experimental flight time differences and Doppler widths for the molecules studied.*

Molecule	Acceleration voltage in the 50eV electrostatic analyzer	TDIFF [a]		WIDTH [a]	
		Calc.	Exp.	Calc.	Exp.
HD	43.7 [b]	-37	-37.5	1	2
HD	37.5 [c]	-7	-9.5	2	3.5
HH	40.6	-19	-21	1	2
DD	40.6	-27	-29	1.5	3

a Given in 200ns units.
b H^+ in time-of-flight channel.
c D^+ in time-of-flight channel.

Table 4. *Kinetic energies and assignments for the coincidence ion spectrum.*

Line no	Kinetic energy (eV)	Assignment	Line no (Larson *et al*)	Kinetic energy (Larson *et al*)
1			1	1.8
2				
3				2.8
4	3.2	$B\,^3\Sigma^-_u \rightarrow O^+(^4S) + O^+(^2P)$	3	3.4 (3.3)
5	4.0	$B\,^3\Pi_g \rightarrow O^+(^4S) + O^+(^2D)$	4	4.5 (4.0)
6	4.6	$A\,^3\Sigma^+_u \rightarrow O^+(^4S) + O^+(^4S)$	4	4.5 (4.3)
7	5.4		5	5.4
8	6.1	$1\,^3\Delta_g \rightarrow O^+(^4S) + O^+(^2D)$	6	6.0 (6.0)

FIGURES

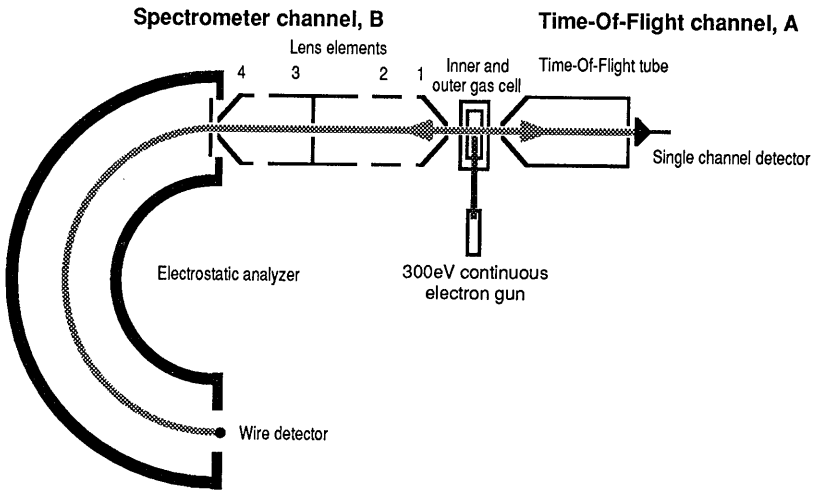

Fig.1. *A schematic drawing of the coincidence instrument.*

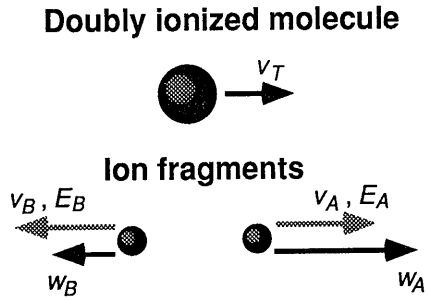

Fig.2. *The notations used for fragment velocities and energies. The grey arrows indicate the center of mass variables, and the black arrows indicate the velocities in the laboratory system.*

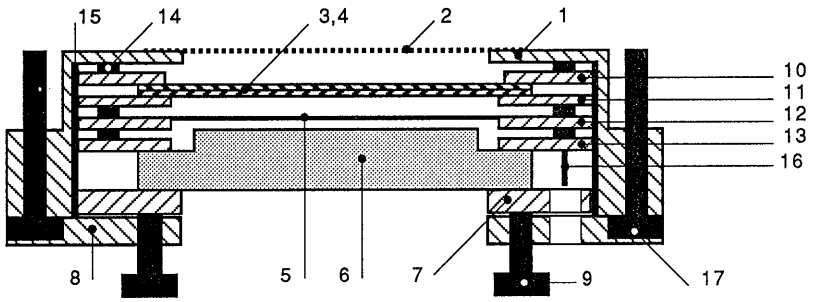

Fig.3. *A schematic cross section of the detector assembly. The numbers are referred to in the text.*

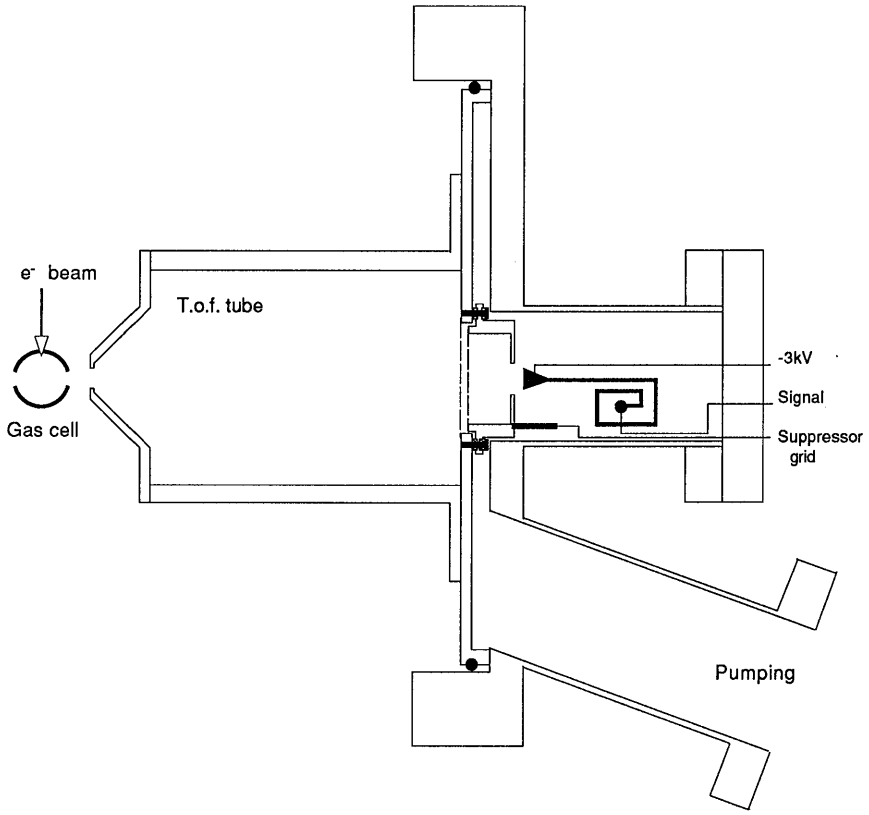

Fig.4. *A schematic drawing of the time-of-flight channel.*

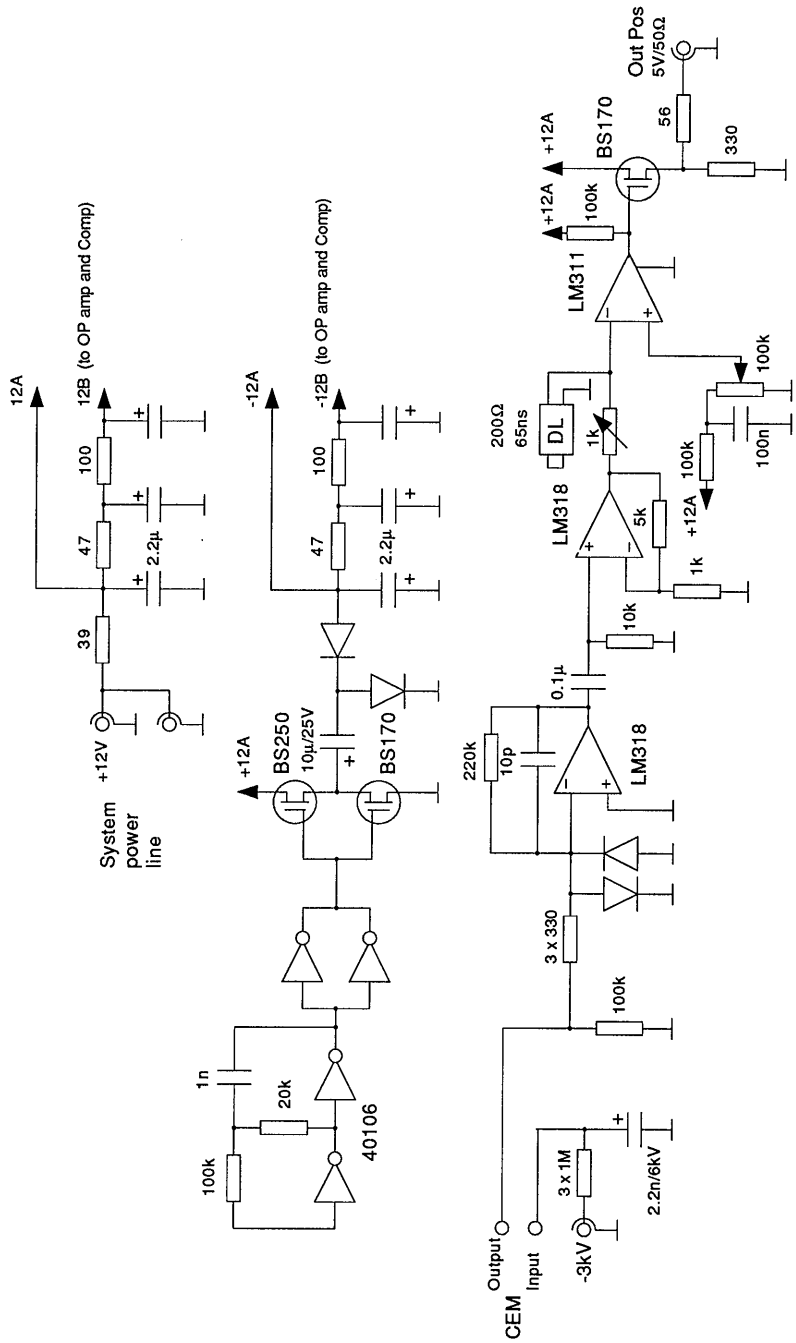

Fig.5. *A circuit diagram of the pre-amplifiers for the wire and channeltron detectors.*

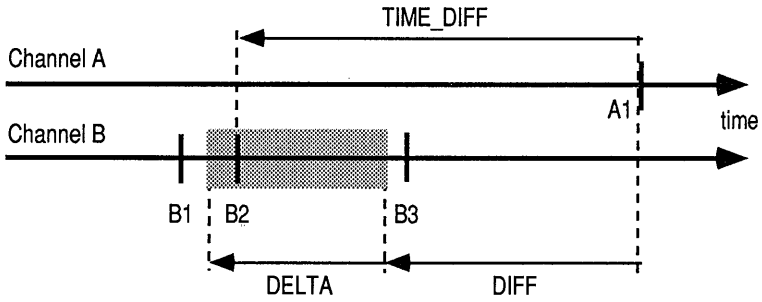

Last event in channel A

Channel A	Channel B
9500	9130
850	8995
0	1138
5001	0
0	15380
598	819
0	0

Last event in channel B

Fig.6. *Top:* *A time diagram showing the parameters used in the coincidence analyzer algorithm, see text.*

Bottom: *The event tables corresponding to the example given in the text.*

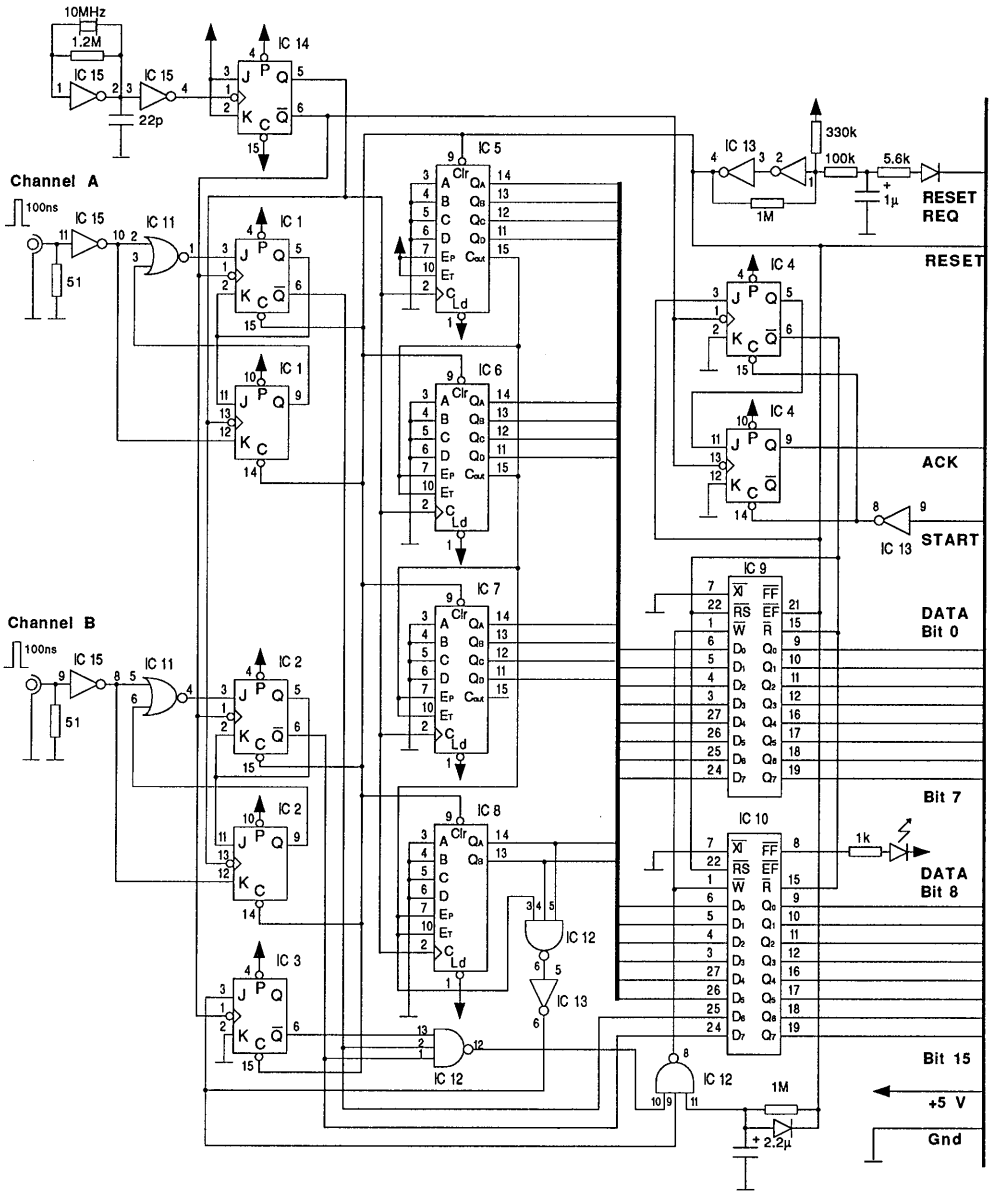

Fig.7. *A circuit diagram of the time base card in the coincidence analyzer .*

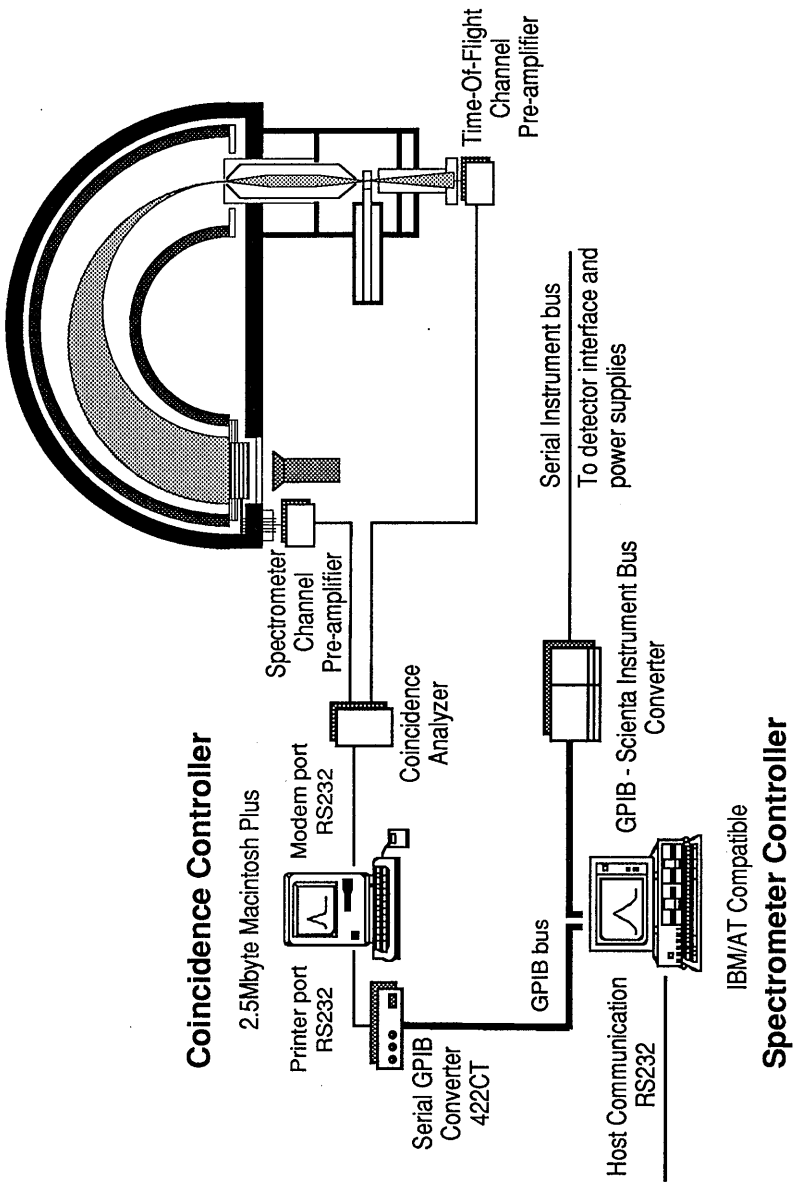

Fig.8. *A system diagram of the coincidence experiment.*

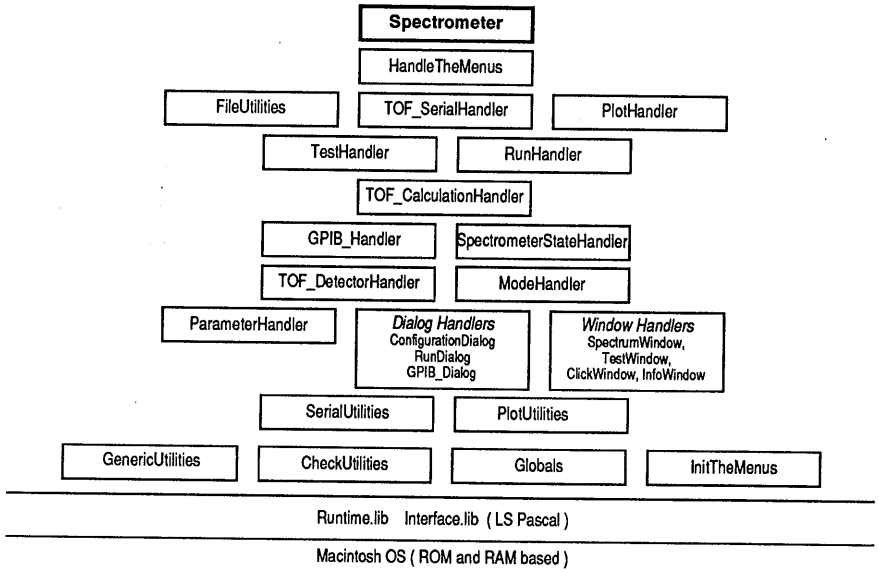

Fig.9. *The software components in the coincidence controller program.*

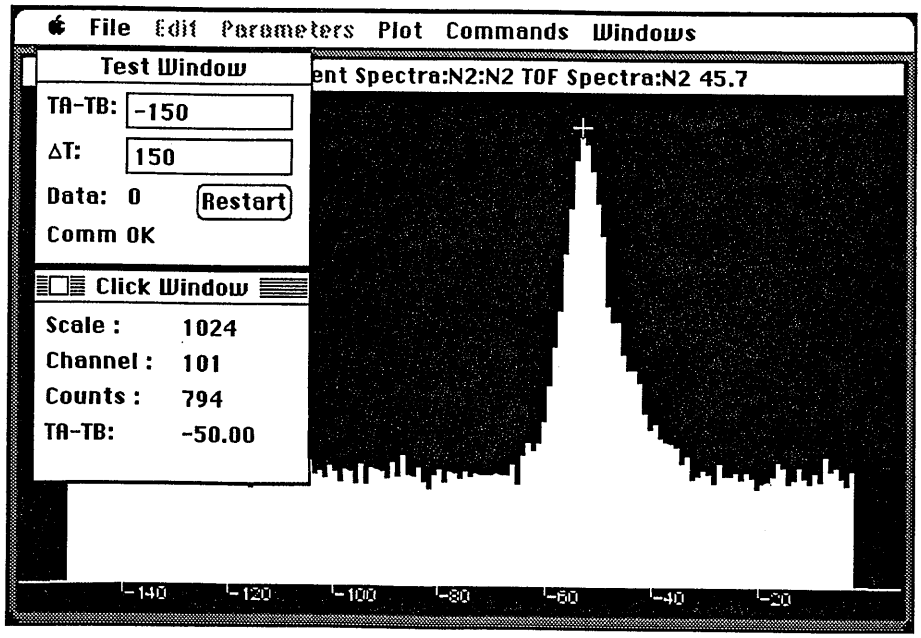

Fig.10. *A screen snapshot of the program operating in the fixed mode running N_2 at a fragment kinetic energy of 4.3 eV.*

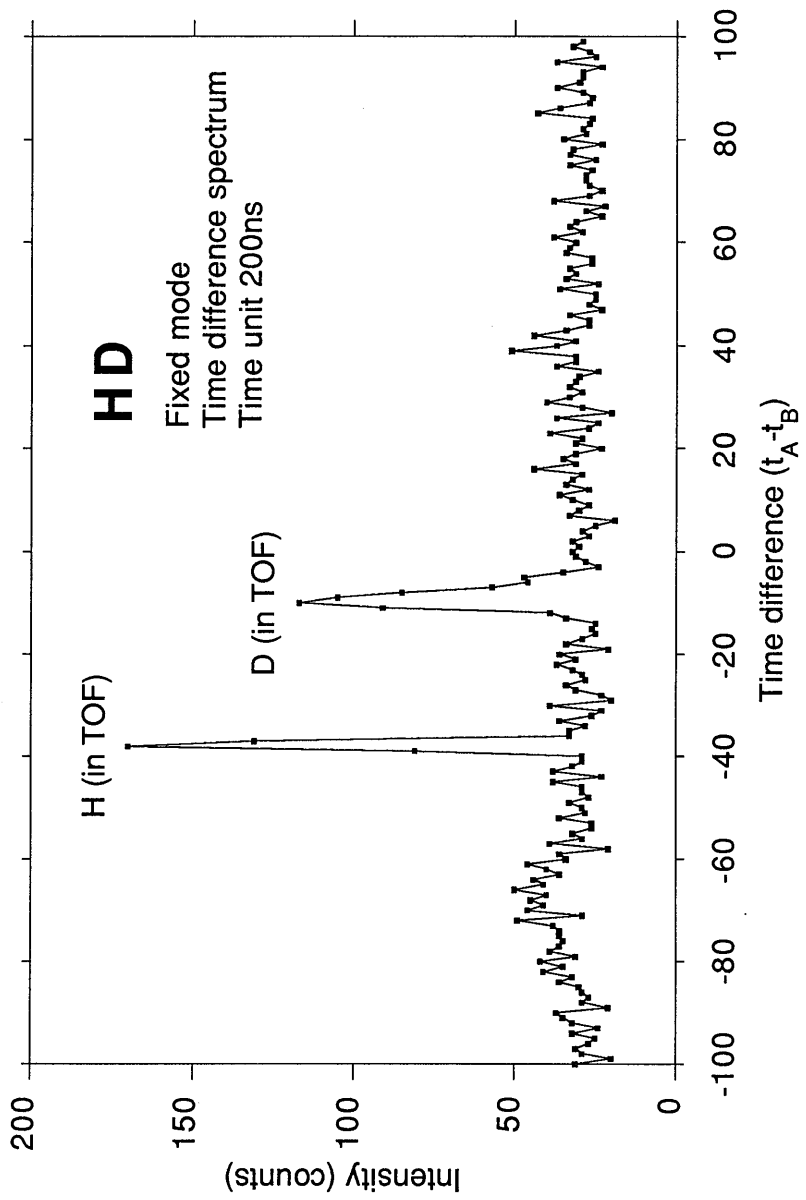

Fig.11. *A fixed mode time difference spectrum of HD. The figure is a combination of two successive recordings with the electrostatic analyzer set to accept either H^+ or D^+ fragments respectively. The spectrometer was set for recording fragments corresponding to a total dissociation energy of 18.8 eV.*

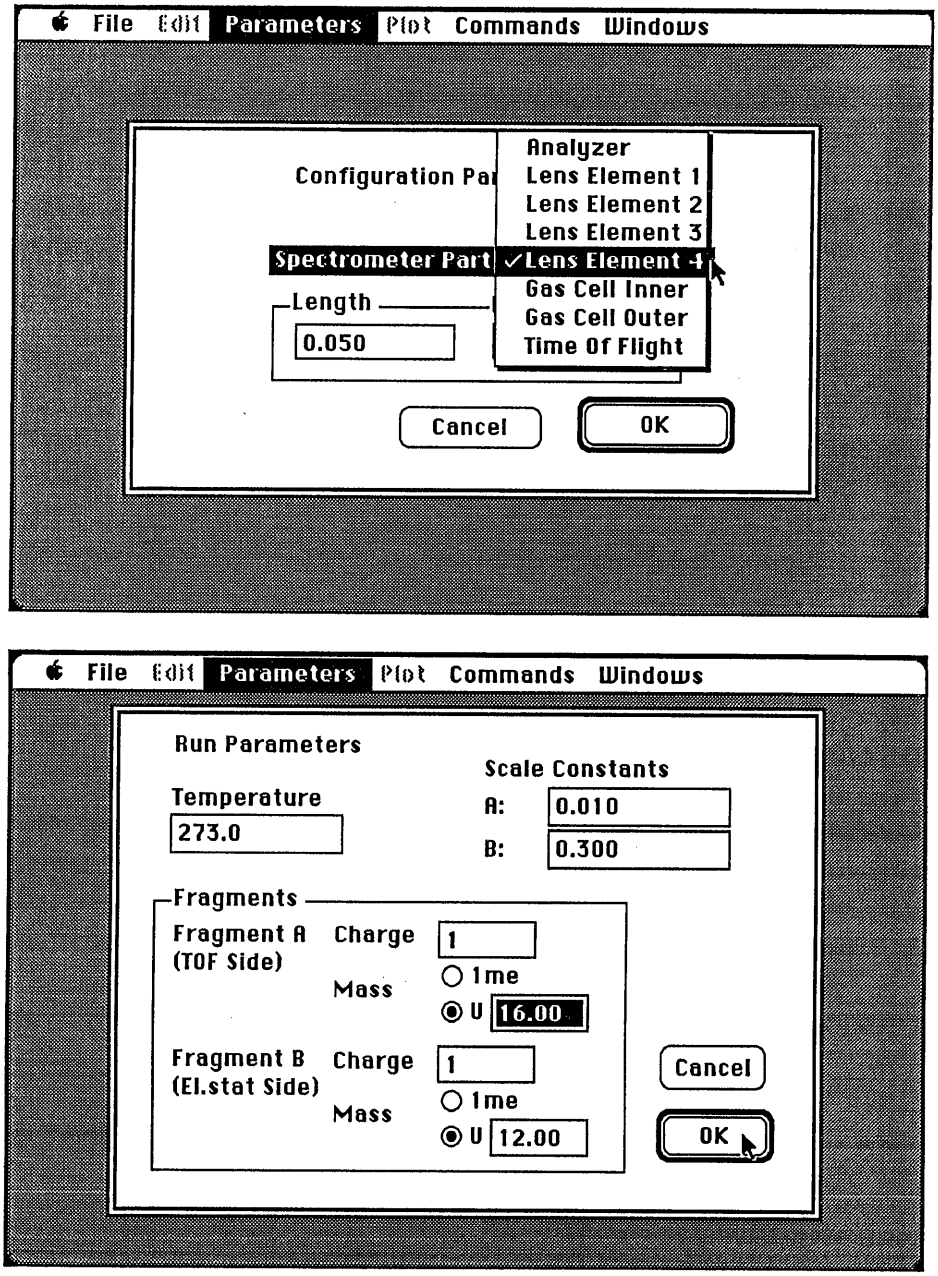

Fig.12. *Top: A screen snapshot of the dialog box in the coincidence controller program used for describing the geometry of the spectrometer.*
Bottom: A screen snapshot of the dialog box used to describe the sample parameters.

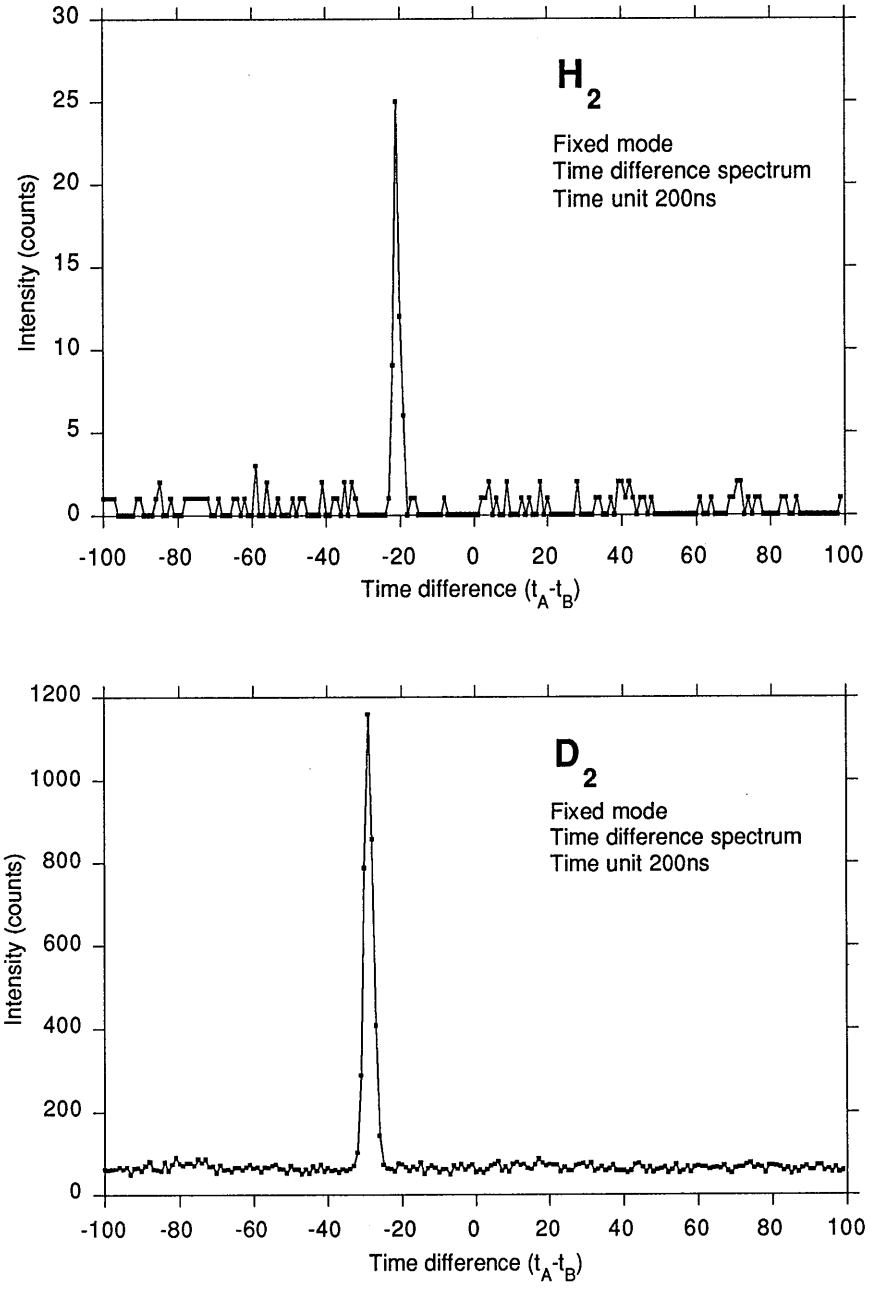

Fig.13. *Fixed mode time difference spectra of H_2 and D_2. The spectrometer was set for recording fragments corresponding to a total dissociation energy of 18.8 eV.*

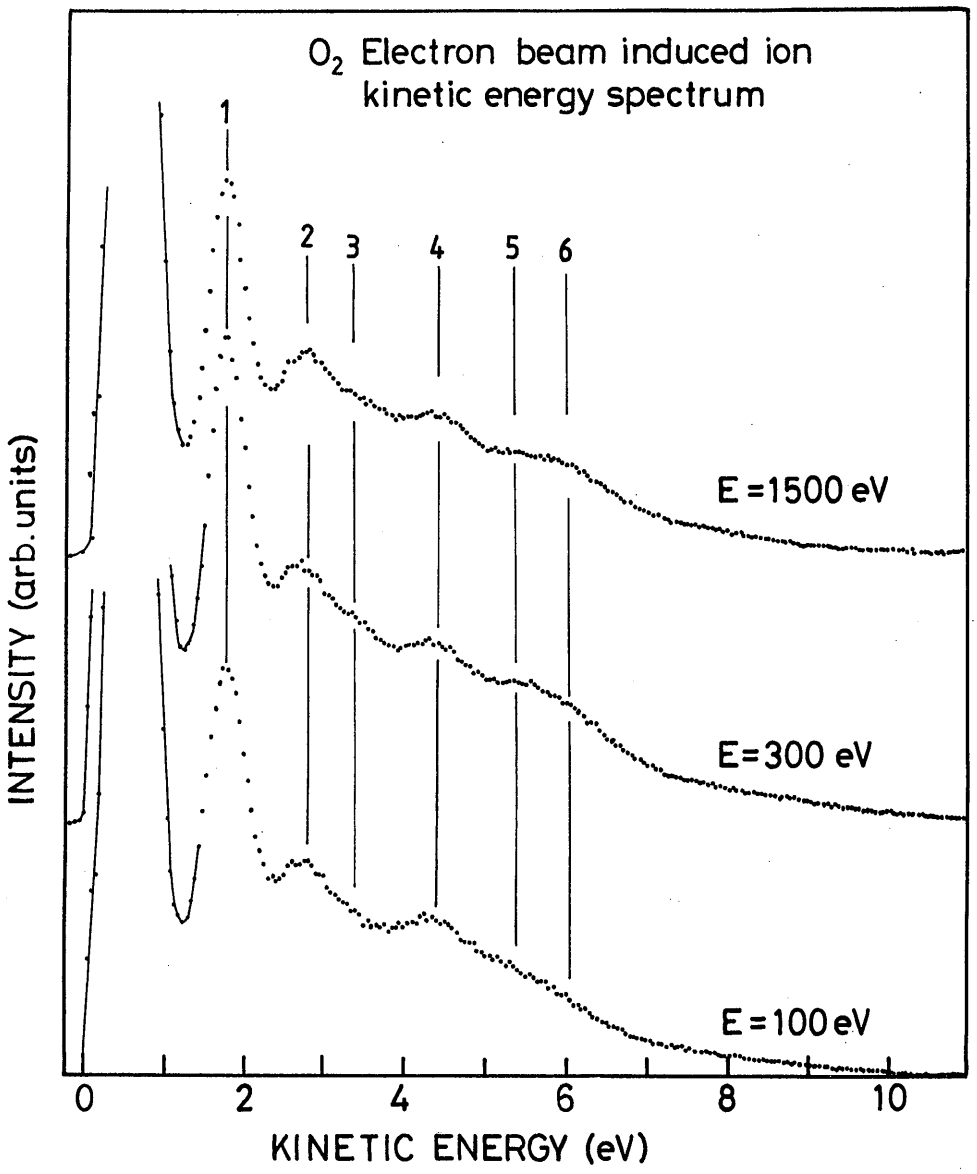

Fig.14. *A swept kinetic energy ion fragment spectrum of O_2^{++} recorded in the electrostatic spectrometer channel alone.*

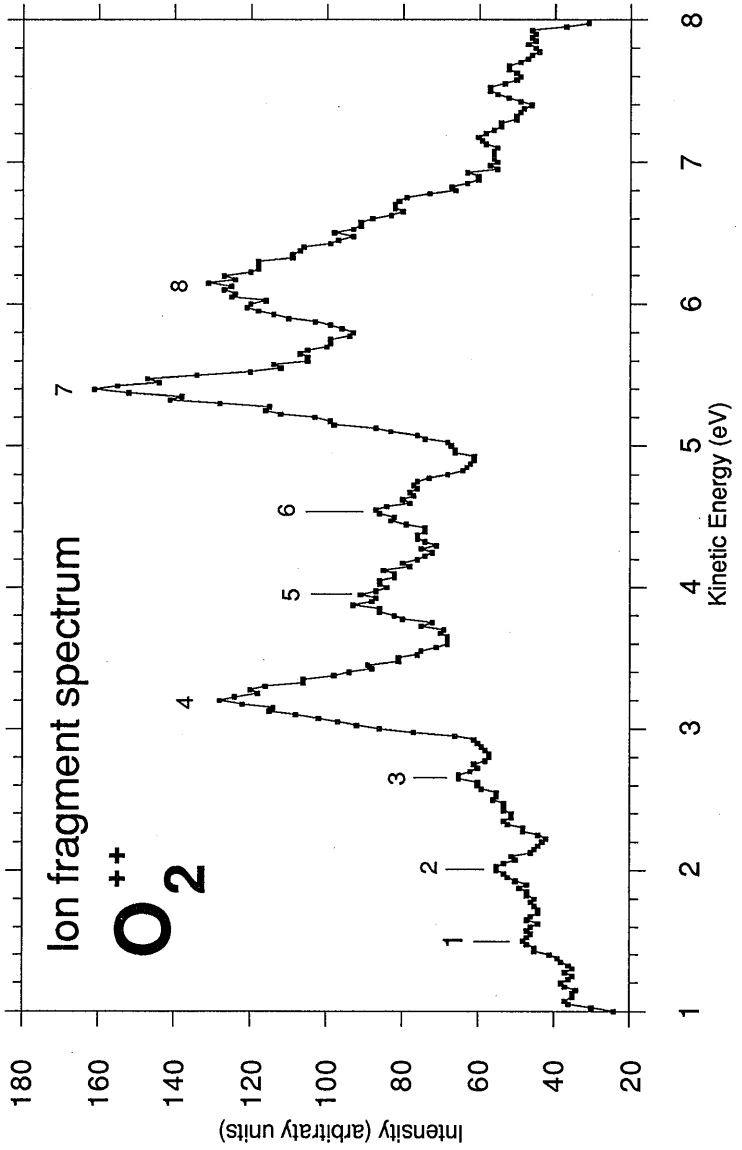

Fig.15. *A swept kinetic energy ion fragment spectrum of O_2^{++} recorded with the coincidence apparatus.*